THE INTRACELLULAR LOCALIZATION OF INORGANIC CATIONS WITH POTASSIUM PYROANTIMONATE

Electron Microscope and Microprobe Analysis

CARLOS J. TANDLER, CÉSAR M. LIBANATI, and CARLOS A. SANCHIS

From the Instituto de Anatomía General y Embriología, Facultad de Medicina, and the Comisión Nacional de Energía Atómica, Buenos Aires, Argentina

ABSTRACT

Potassium pyroantimonate, when used as fixative (saturated or half-saturated, *without* addition of any conventional fixative) has been demonstrated to produce intracellular precipitates of the insoluble salts of calcium, magnesium, and sodium and to preserve the general cell morphology. In both animal and plant tissues, the electron-opaque antimonate precipitates were found deposited in the nucleus—as well as within the nucleolus—and in the cytoplasm, largely at the site of the ribonucleoprotein particles; the condensed chromatin appeared relatively free of precipitates. The inorganic cations are probably in a loosely bound state since they are not retained by conventional fixatives. The implications of this inorganic cation distribution in the intact cell are discussed in connection with their anionic counterparts, i.e., complexing of cations by fixed anionic charges and the coexistence of a large pool of inorganic orthophosphate anions in the nucleus and nucleolus.

INTRODUCTION

The organic cations (Mg^{++}, Ca^{++}, Na^{+}, K^{+}) are known to be important constituents of all living animal and plant cells (1). However, little is yet known about their distribution at the intracellular level.

The same was true for the orthophosphate ion, which generally constitutes the bulk of the inorganic anions within the cell (1). Previous work in our laboratory demonstrated that it is possible to localize this water-soluble electrolyte at the subcellular level with the electron microscope (2); further information was gained through the application of the microprobe (3). The results indicated that the inorganic phosphate ions are accumulated in the nucleus with the nucleolus showing the highest concentration of this electrolyte (2, 3).

Because of the high level of inorganic phosphate within the nucleus, as reported in those papers, a high concentration of cations as counter-ions and with a similar distribution was predicted for the cell nucleus (2, 3). In order to investigate this point, we used an approach similar to that employed for the phosphate anion, but with potassium pyroantimonate as the precipitating reagent for the cations.

Komnick (4) was the first to use this reagent mixed with osmium tetroxide fixative in an attempt to localize sodium ions. His procedure was followed by all subsequent investigators (as such

or slightly modified, 5–13). Electron-opaque antimonate deposits have been localized in both the cytoplasm and the nucleus; particularly heavy deposits were found in the nucleolus by Spicer et al. (10). The deposits were attributed presumably to a precipitate of sodium pyroantimonate, although it has been pointed out that the solubility characteristics of calcium and magnesium pyroantimonates, among other salts, are such that these salts may also form electron-opaque particles in the tissue (5, 13). Furthermore, in the absence of a direct chemical identification it cannot be decided whether the deposits are due to a deposition of the potassium pyroantimonate itself or to a precipitation reaction with the cellular cations.

In the present paper, we report a new and simple procedure based on the use of potassium pyroantimonate *alone* as a fixative (i.e., without addition of any other conventional fixative). Combined electron microscope and microprobe analysis conclusively demonstrates that upon immersion of unfixed tissues in an aqueous solution of that reagent, the cell morphology was strikingly well preserved and insoluble antimonate compounds containing Ca, Mg, and Na precipitated massively inside the nucleus and nucleolus as well as in the cytoplasm. The implications of this compartmentalization in the intact cell are discussed in connection with the anionic counterparts for these cations.

MATERIALS AND METHODS

The investigations were carried out on vigorously growing maize roots, the radicle of ungerminated broad bean embryos, and rat liver. The maize roots which developed upon contact with tap or twice distilled water were cut and fixed. The ungerminated radicle was dissected out from the broad bean seeds and immersed in the fixative. Rats were killed by decapitation, and small slices of liver about 1 mm thick were immediately fixed.

Electron Microscope Fixation Procedure

Potassium pyroantimonate (Riedel-De Haën Ag., Seelze, Hanover, Germany, analytical reagent) was employed. A saturated solution in water (about 2%, w/v) was always freshly prepared by boiling the potassium pyroantimonate in deionized or twice glass-distilled water, cooled rapidly to room temperature, and centrifuged.

This solution was first used mixed with osmium tetroxide either according to Komnick (4, 5) or as described by Spicer et al. (10). However, it was soon found that when potassium pyroantimonate *alone* is used as fixative, the general morphology of the cell is strikingly well preserved and large amounts of antimonate precipitates are retained within the tissue and cells. Therefore, the present study has been made exclusively with this new and simple procedure. The fixatives used were: (*a*) saturated potassium pyroantimonate (pH about 9.2); (*b*) half-saturated potassium pyroantimonate, prepared by mixing equal volumes of the saturated solution and of twice distilled water; and (*c*) same solution as *a*, but adjusted to pH 8.2 by addition of a few drops of glacial acetic acid. In *c*, a voluminous precipitate forms on addition of each drop and the pyroantimonate solution is centrifuged each time before checking the pH; the amount of pyroantimonate ion remaining in solution has not been determined. A point to be stressed is that on further addition of acid (acetic or HCl) even more antimonate comes out of the solution and that when the pH reaches neutrality, or slightly below it, little or no pyroantimonate anions remain soluble; this solution does not precipitate at all with inorganic cations. The precipitate formed by addition of acids is probably the potassium pyroantimonate itself, since it can be dissolved again by washing the acid with cold twice distilled water and thereafter heating in distilled water.

The time of fixation was 6–12 hr (usually overnight) at room temperature.

Washings and Embedding

After fixation, the tissues were hardened by placing them in a 5% formaldehyde solution in potassium pyroantimonate for 6–24 hr at room temperature. This reagent was always freshly prepared by addition of 1 volume of 40% formaldehyde (free of acid, Merck, Darmstadt, Germany) to 7 volumes of the saturated solution of potassium pyroantimonate; a small amount of precipitate forms which is eliminated by centrifugation. This precipitate is probably due to the acid pH (about 5.3) of the formaldehyde reagent, since it redissolves again after washing and heating in distilled water or in half-saturated potassium pyroantimonate (i.e., its behavior resembles the precipitate obtained by addition of acids to the pyroantimonate solution). The tissues were afterwards washed for 30 min with two or three changes of deionized or twice distilled water at room temperature.

Alternatively, after hardening with the above-described formaldehyde solution, the tissues were transferred to a half-saturated solution of potassium pyroantimonate, heated at 90–95°C for 5 min, rapidly cooled, and then washed with ice-cold twice-distilled water. This step was used in an attempt to solubilize any precipitated or adsorbed potassium pyroantimonate. The sodium, calcium, magnesium, zinc, and iron pyroantimonates are insoluble in hot

distilled water; heating with a half-saturated potassium pyroantimonate solution decreases even more the solubility of these insoluble pyroantimonates as a result of the common-ion effect. Therefore, there is no risk that those pyroantimonate precipitates will be washed out of the tissue, even by a prolonged heating of the tissue.

In the present study, postosmication—and staining as well—was always *omitted* in order to correlate all the electron opacity observable in the electron micrographs (Figs. 1–6) to the presence of antimony (as insoluble pyroantimonate precipitates).

After the tissues were washed, they were dehydrated with graded concentrations of cold ethanol, passed through propylene oxide, and embedded in Maraglas (Marblette Corp., Long Island City, N. Y.). It was found necessary to extend to 12–24 hr the time of immersion in the propylene oxide-Maraglas mixture and in Maraglas in order to assure a good penetration of the plastic. Thin sections were cut with glass knives on a Porter-Blum microtome, mounted on Formvar-coated copper grids, and examined *unstained* with a Siemens Elmiskop I electron microscope. Thick (1 μ) sections were also cut, fastened to a microscopic slide, and stained with polychrome blue in 0.1% sodium carbonate for examination under the light microscope.

Electron Microprobe

The distribution of the atomic elements in the thick (1 μ) sections was studied with a Cameca model MS 46 X-ray microanalyzer with an accelerating voltage of 10 kv for the lighter elements (Na, Mg, Ca) and 30 kv for antimonium and a probe current of 70–100 nA. The L α_1-radiation was used for antimony while the lighter elements were scanned with the K α_1-radiation. The preparation of the specimen, which is a simple one, has been described (3). The relative distribution of these elements was recorded in micrographs (e.g., Figs. 8–10), and their topography can be correlated with the absorbed electron image (Fig. 7) of the same area. The number of white specks in a micrograph is proportional to the concentration of the element present at different points in the *same* micrograph. It must be emphasized that the different micrographs are not quantitatively comparable, since the conditions of analysis are not similar; therefore, the relative proportions of the different cations cannot be judged in this way.

It is to be noted that the maize root was selected for this work because of the relatively large size of the nucleoli which may reach more than 5 μ in diameter; this fact permits their analysis with the microprobe (see also references 2, 3). On the other hand, a resolution of the nucleoli in the normal hepatocyte nucleus is not possible with the probe.

RESULTS

Electron Microscope

The most prominent feature to be observed in unstained sections of pyroantimonate-fixed tissues is the presence of abundant electron-opaque deposits (Figs. 1–6). These deposits were not altered by heating the tissues at 90–95°C in half-saturated potassium pyroantimonate (either before or after the formaldehyde-hardening step), strongly suggesting that they are not composed of potassium pyroantimonate exclusively. Those deposits remained equally insoluble when the heating procedure was performed with the thin sections mounted on copper grids; even heating in twice-distilled water does not remove them. Therefore, this electron-opaque material must have originated from a precipitation reaction between the pyroantimonate anions of the fixative and the cellular cations. This point is clearly demonstrated with the microprobe analysis (see below).

Fig. 1 shows an unstained section of maize root fixed in saturated potassium pyroantimonate, about 5 mm from the tip; these cells are highly vacuolized, and the cellulose walls have collapsed during the dehydration procedure. The electron-opaque antimonate precipitates are massively deposited in the large nucleolus and in much lesser amounts in the rest of the nucleus. The nucleolus boundary is quite sharply delimited by the precipitates. At higher magnifications, these antimonate deposits are seen as "granules" about 400 A in diameter, and are apparently formed by aggregation of smaller granules. The cellulose walls and the middle lamellae show a finely granular precipitate; a "layer" of a more concentrated precipitate, measuring roughly 300 A thick, delimits the cytoplasmic boundaries with the cellulose walls. A densely packed granular precipitate is found at some places in the intercellular spaces, e.g., the triangular schizogenous spaces (Fig. 1). In this material, similar results were obtained when a half-saturated solution of potassium pyroantimonate or a solution of the same salt adjusted to pH 8.2 was used as fixative.

Fig. 2 shows the distribution of the antimonate precipitates in a thin section from the radicle of broad bean seed fixed in saturated potassium pyroantimonate. The ungerminated embryo was chosen in order to compare the cation distribution in a physiologically dormant radicle (Fig. 2) with that of a growing, functional root (Fig. 1); more-

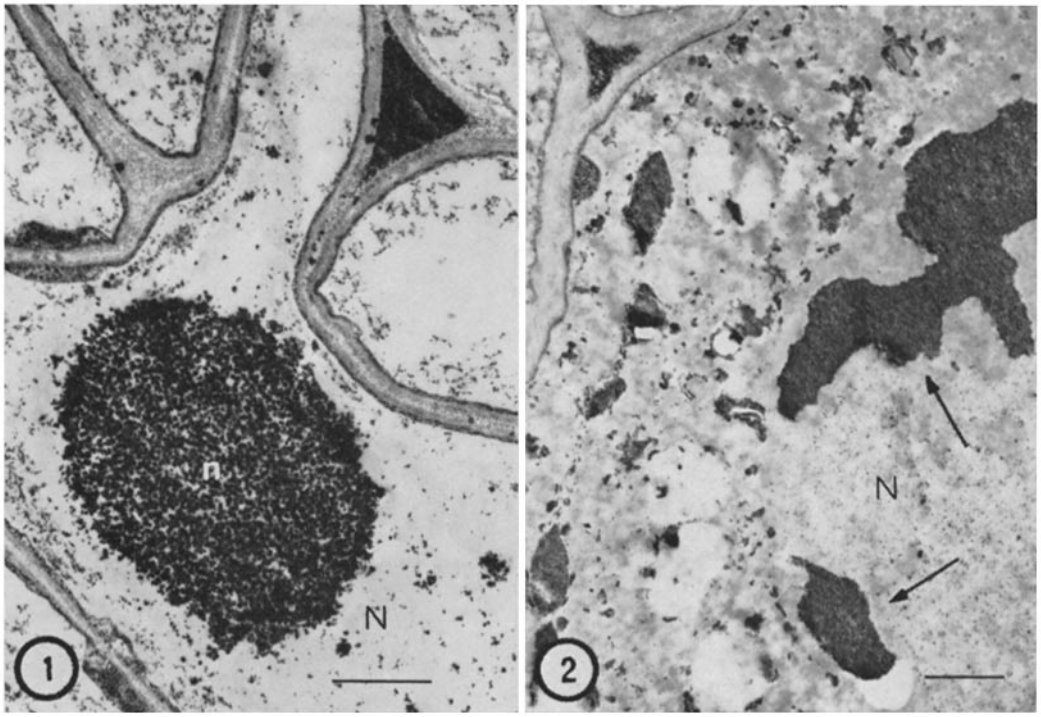

In all the electron micrographs shown in these figures, the tissues have been fixed in potassium pyroantimonate alone without addition of any conventional fixative, hardened with formaldehyde, and embedded in Maraglas. Postosmication and staining were always *omitted*.

FIGURE 1 Electron micrograph of a portion of a vacuolized maize root cell and its nucleus (*N*), illustrating the massive deposition of electron-opaque precipitates in the nucleolus (*n*), in the triangular schizogenous space, and at the cytoplasmic boundary with the cellulose walls. A finely granular precipitate appears in the cellulose walls and middle lamellae. Fixation: saturated potassium pyroantimonate. Scale mark, 1 μ. × 13,000.

FIGURE 2 Thin section of a radicle from the broad bean seed fixed as for Fig. 1. The pyroantimonate precipitate is localized in the nucleoli (arrows), in several unidentified cytoplasmic bodies, at the cell wall, and in the schizogenous space. *N*, nucleus. Scale mark: 1 μ. × 10,500.

over, that tissue is highly dehydrated and, therefore, the only water put in contact with the cell contents is that of the fixative. As can be seen in Fig. 2, massive electron-opaque precipitates are also found in the nucleoli and at some places in the intercellular spaces (e.g., the triangular schizogenous spaces) while a fine granular precipitate is evidenced in the cellulose walls, especially at the boundaries with the cytoplasm. This pattern of pyroantimonate deposition is similar to that of the functional root (Fig. 1). In the broad bean radicle, several massive antimonate deposits of different sizes also can be seen in the cytoplasm (Fig. 2). A sequential thick (1 μ) section stained with polychrome blue and observed with the light microscope confirmed that these nuclei have multiple nucleoli similar in shape and size to those observed in the electron micrograph of Fig. 2 and, furthermore, that the dense unidentified cytoplasmic bodies are also heavily stained.

A point of interest is that the massive antimonate precipitates in Fig. 2 are more finely granular than those of Fig. 1, a fact that could be due to the dehydrated condition of the radicle.

Fig. 3 shows a survey electron micrograph of an unstained section of rat liver fixed in half-saturated potassium pyroantimonate. The electron-opaque antimonate precipitates are massively deposited

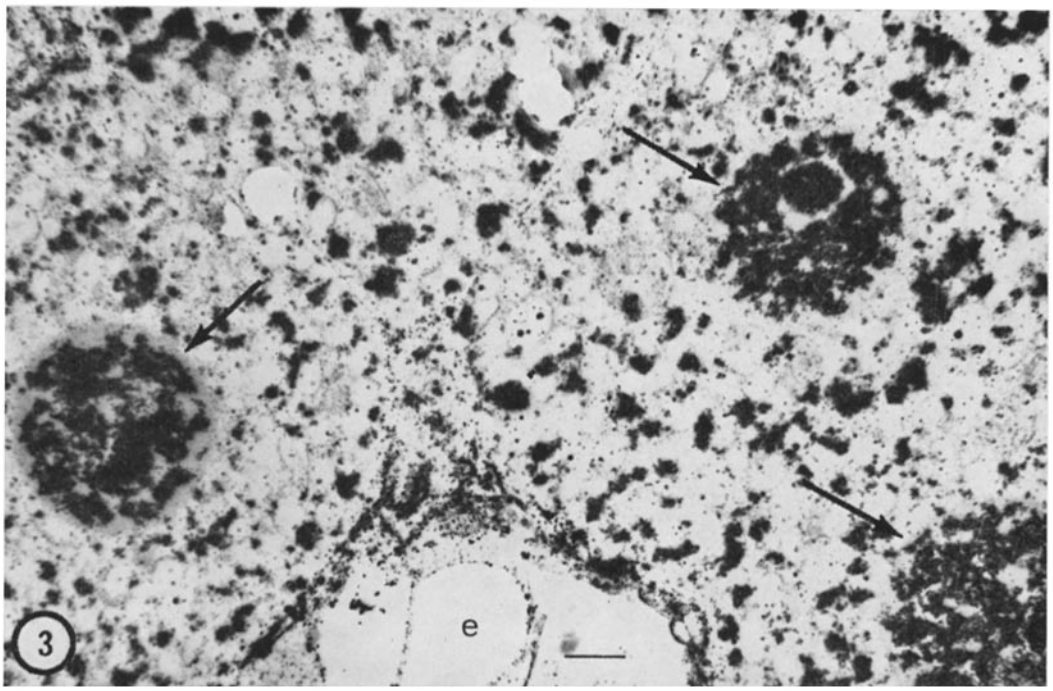

FIGURE 3 Survey electron micrograph of a thin section of rat liver fixed in half-saturated potassium pyroantimonate, illustrating the generality of the reaction. The precipitates are localized in the nuclei (arrows), in several discrete masses in the cytoplasm, and in the wall of the blood vessel; *e*, erythrocyte. Mark, 2 μ. × 4,000.

within the nucleus and nucleolus, in several discrete masses in the cytoplasm and in the blood vessel walls. A sequential thick (1 μ) section stained with polychrome blue and observed with the light microscope indicates that the antimonate sites of precipitation in the cytoplasm appear to correspond to the sites of the ribonucleoprotein distribution. In the nulecus, the pattern of antimonate deposition does not correlate with that of the condensed chromatin; this can be easily seen in the chromatin lying against the nuclear membrane and around the nucleolus, which is largely free of precipitate. This pattern of antimonate deposition in the nucleus is also directly observed in the electron micrograph of Fig. 4 taken at higher magnification in which the condensed chromatin at these two sites can be discerned because of its intrinsic electron opacity. At higher magnifications, the precipitates in the nuclei are seen as spherical aggregates, about 600 A in diameter, denser at their periphery. The absence of this granular precipitate in the condensed chromatin is also illustrated in Fig. 5, which shows a leukocyte inside a small blood vessel and an endothelial nucleus. The antimonate precipitates are morphologically similar to those of the hepatocyte nuclei and are evidently dispersed between the condensed masses of chromatin. Although one would expect divalent cations also to be associated with sites of high DNA content, the present results appear to indicate that the condensed chromatin in the interphase nucleus is largely free of ionizable cations (i.e. those precipitable with potassium pyroantimonate). The presence of chelated cations cannot be ruled out since they will not yield insoluble pyroantimonate salts; this apparently is the case for iron in hemoglobin, the red cells being largely free of precipitates (Fig. 3). A finely nonaggregated precipitate can be seen dispersed within the whole nucleus (Fig. 5) or cytoplasm (Figs. 3 and 5), but it is not clear whether this reflects a low concentration of cations at these sites or traces of the fixative which resisted the washing procedure.

A correlation between both the distribution and the amount of inorganic cations with that of the

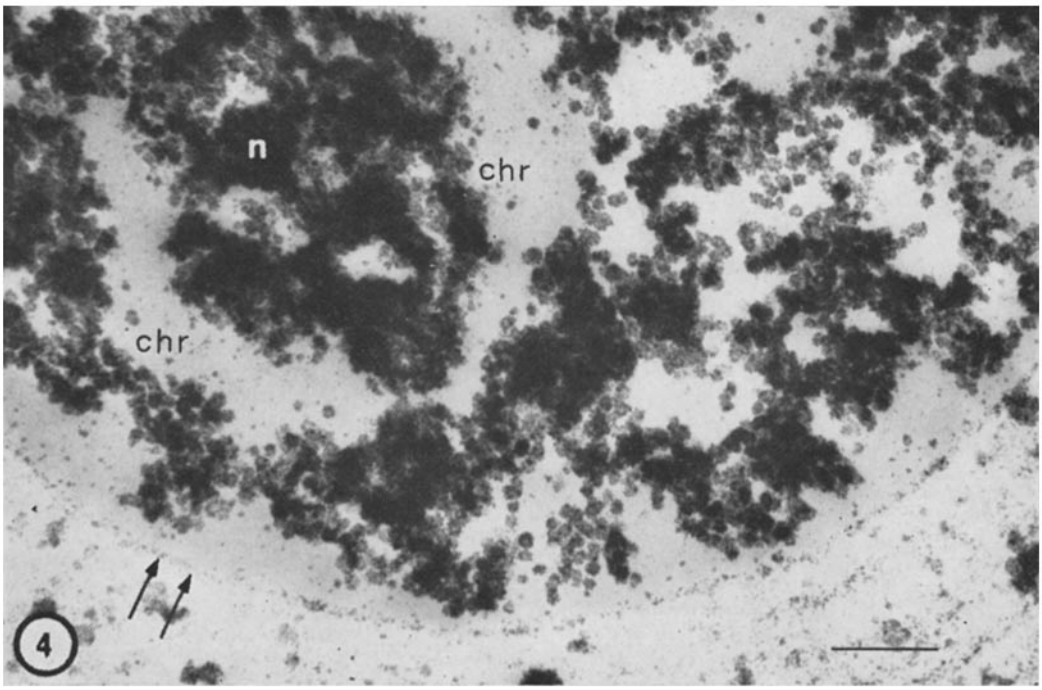

FIGURE 4 Electron micrograph of part of a rat liver cell nucleus; fixation as for Fig. 3. The condensed chromatin (*chr*) associated with the nucleolus (*n*) and the nuclear membrane (double arrow) are relatively free of precipitate which is massively deposited in the nucleolus and in the rest of the nucleus. Mark, 0.5 μ. × 28,500.

ribonucleoprotein particles seems evident for the cell nucleus. This statement is based on the comparison of the granular aggregate precipitates in the two types of nuclei (Figs. 4 and 5) with the figures published recently by Monneron and Bernhard (Figs. 1 and 2 in reference 14) showing the topography of ribonucleoprotein in these nuclei. Both the ribonucleoprotein particles and the inorganic cations are abundant in the hepatocyte, are relatively scarce in the leukocyte, and are dispersed between the condensed chromatin. The nucleolus, which is well known to be rich in ribonucleoprotein, also shows a heavy precipitate of insoluble antimonate salts (Figs. 4 and 1).

Fig. 6 shows a "projection" of pyroantimonate precipitate towards the nuclear membrane; on the cytoplasmic side of it a massive precipitate of pyroantimonate protrudes into the cytoplasm and has an appearance similar to that of the cytoplasmic antimonate deposits found in the basophilic masses of ribonucleoprotein. This observation strongly suggests that this area is coincident with a pore in the nuclear membrane and that what is observed is part of the processes taking place during the passage of ribonucleoprotein into the cytoplasm; whether this passage is also accompanied by the cations cannot be decided on morphological observations alone.

At relatively low magnifications, the morphologies of the antimonate precipitates in the nucleus and cytoplasm seem to differ considerably; however, at high magnifications, spherical granular aggregates denser at the periphery can be visualized in the cytoplasm, although they are more tightly packed than in the nucleus (Fig. 6).

Massive precipitates of insoluble salts are found in the walls of all the blood vessels; inside them, the precipitate is located in the plasma and inside the leukocytes. The boundary between two adjacent hepatocytes is generally delimited by a deposition of an antimonate precipitate about 300–400 A thick and probably corresponds to the opposed cell membranes.

The electron-opaque precipitates of Figs. 1–6 are absent in tissues fixed for 2.5 hr in 2% glutaraldehyde, 5% formaldehyde, 5% cold trichloroacetic

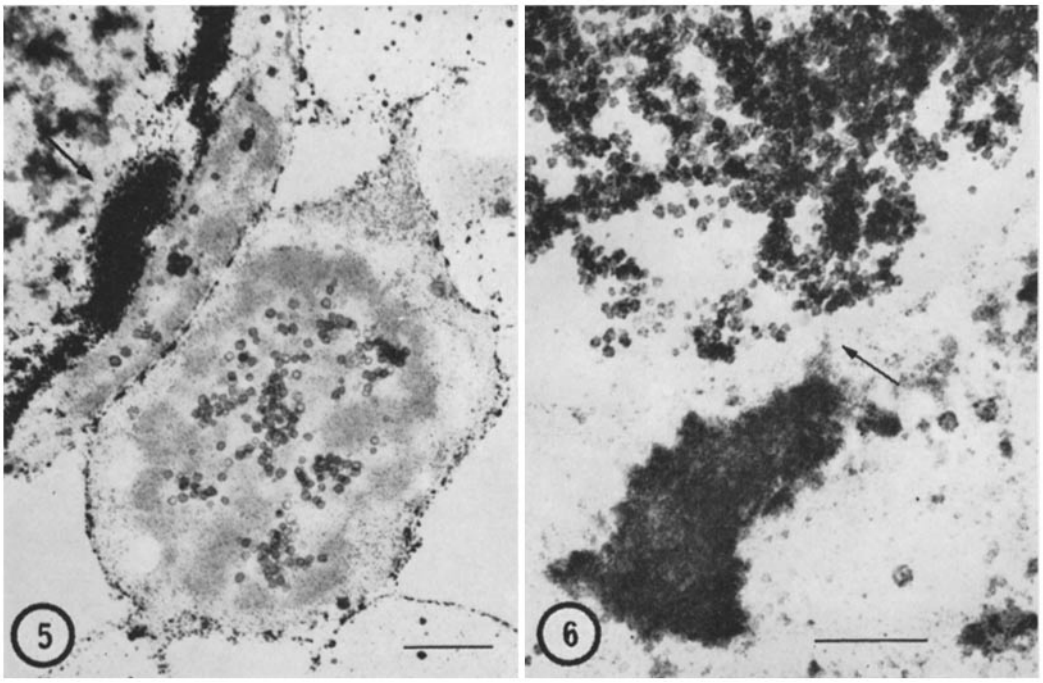

FIGURE 5 Thin section of a lymphocyte in a small blood vessel of rat liver fixed as for Fig. 3. The precipitate is scarcer than in the hepatocyte nucleus and is also dispersed between the masses of chromatin. A nucleus of an endothelial cell is discernible at the left of the leukocyte. A massive precipitate is localized in the wall of the blood vessel (arrow). Mark, 1 μ. × 12,000.

FIGURE 6 Electron micrograph of a portion of the nucleus and cytoplasm of rat liver fixed as for Fig. 3. In the cytoplasm, a massive pyroantimonate precipitate in contact with the nuclear membrane (arrow) is apparent. Mark, 1 μ. × 15,000.

acid, or 1% osmium tetroxide, washed with twice distilled water, and immersed afterwards in potassium pyroantimonate. This indicates that the cellular cations are easily leached out of the cells and could not be satisfactorily retained by the conventional fixatives. In the intact cell, a large part of the cations are apparently in a relatively loosely "bound" state, in the sense that they are easily solubilized (and washed out) by distilled water following the alterations produced by the chemical fixatives. This last statement is made more evident when the conventional fixatives (2% glutaraldehyde, 5% formaldehyde, 1% potassium permanganate, 1% potassium dichromate) are added to the saturated or half-saturated potassium pyroantimonate solution and then tested. These mixed fixatives do not affect precipitation of sodium, calcium, and magnesium in the test tube; however, they cause a rapid diffusion and leakage of cations from cells and tissues as judged by the scarcity of the electron-opaque precipitates, and negative results were commonly obtained. This fact stands in great contrast to the results obtained with the potassium pyroantimonate solution alone. It is evident, therefore, that our procedure does preserve a significant proportion of inorganic cations inside the cells and tissue and at the subcellular level. Addition of 1% osmium tetroxide to the potassium pyroantimonate solution resulted in electron-opaque deposits in the nuclei and in some other sites in the tissues, as found by other authors (5–13); however, they were much less abundant than with potassium pyroantimonate alone.

Electron Microprobe

Figs. 7 and 11 show the absorbed electron image taken with the microprobe from thick 1 μ sections of potassium pyroantimonate-fixed maize root and rat liver, respectively. In Fig. 7, the

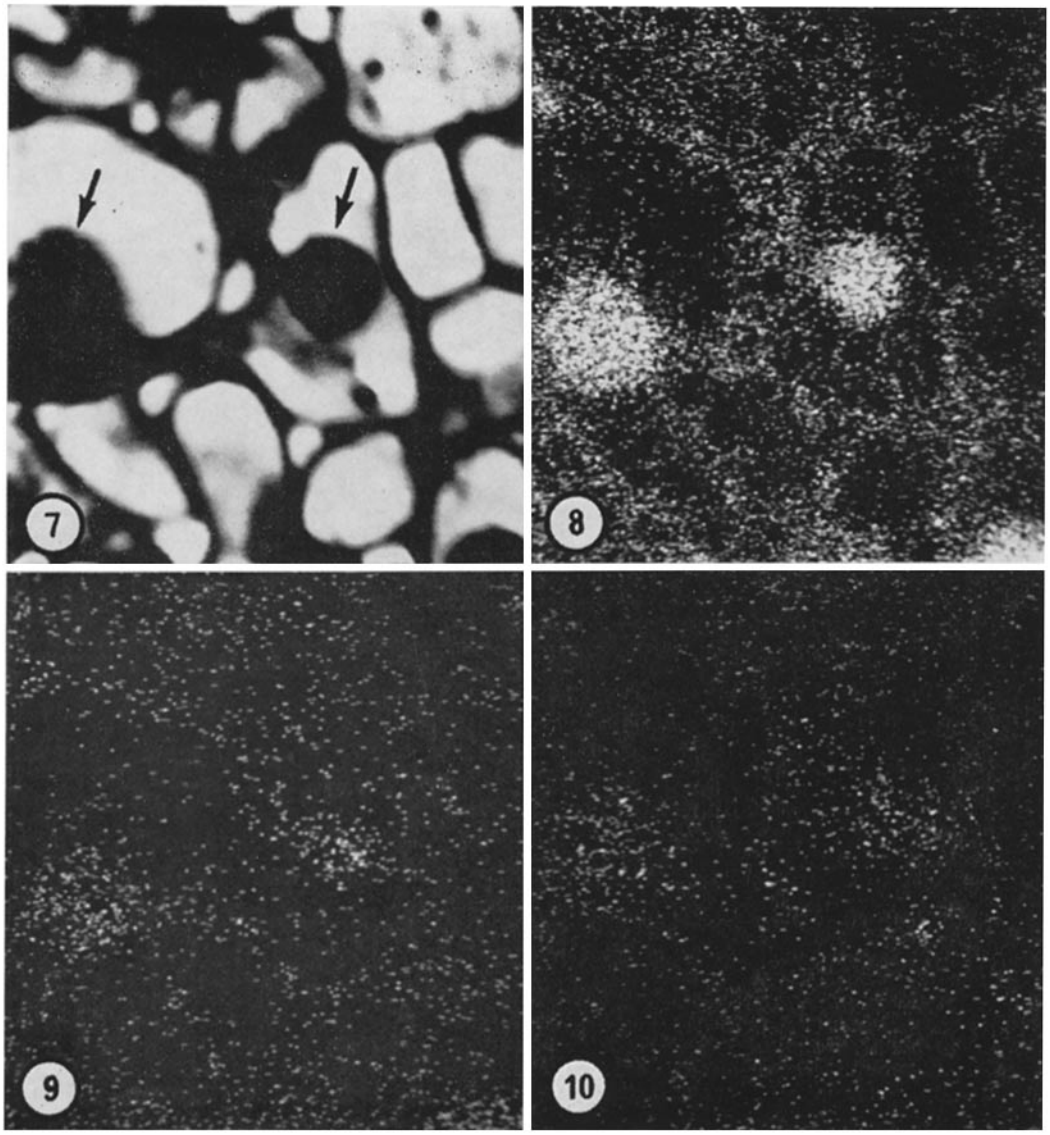

FIGURE 7 Absorbed electron image taken with the microprobe from a thick 1 μ section of maize root fixed in potassium pyroantimonate. The outlines of two nucleoli (arrows) and of the cell walls are evident. × 2,300.

FIGURE 8 The image for the Lα_1-emission wavelength of antimony on the same area of the section shown in Fig. 7. × 2,300.

FIGURE 9 The image for the Kα_1-emission wavelength of magnesium on the same area of the section shown in Figs. 7 and 8. × 2,300.

FIGURE 10 The image for the Kα_1-emission wavelength of calcium on the same area of the section shown in Figs. 7 and 8. × 2,300.

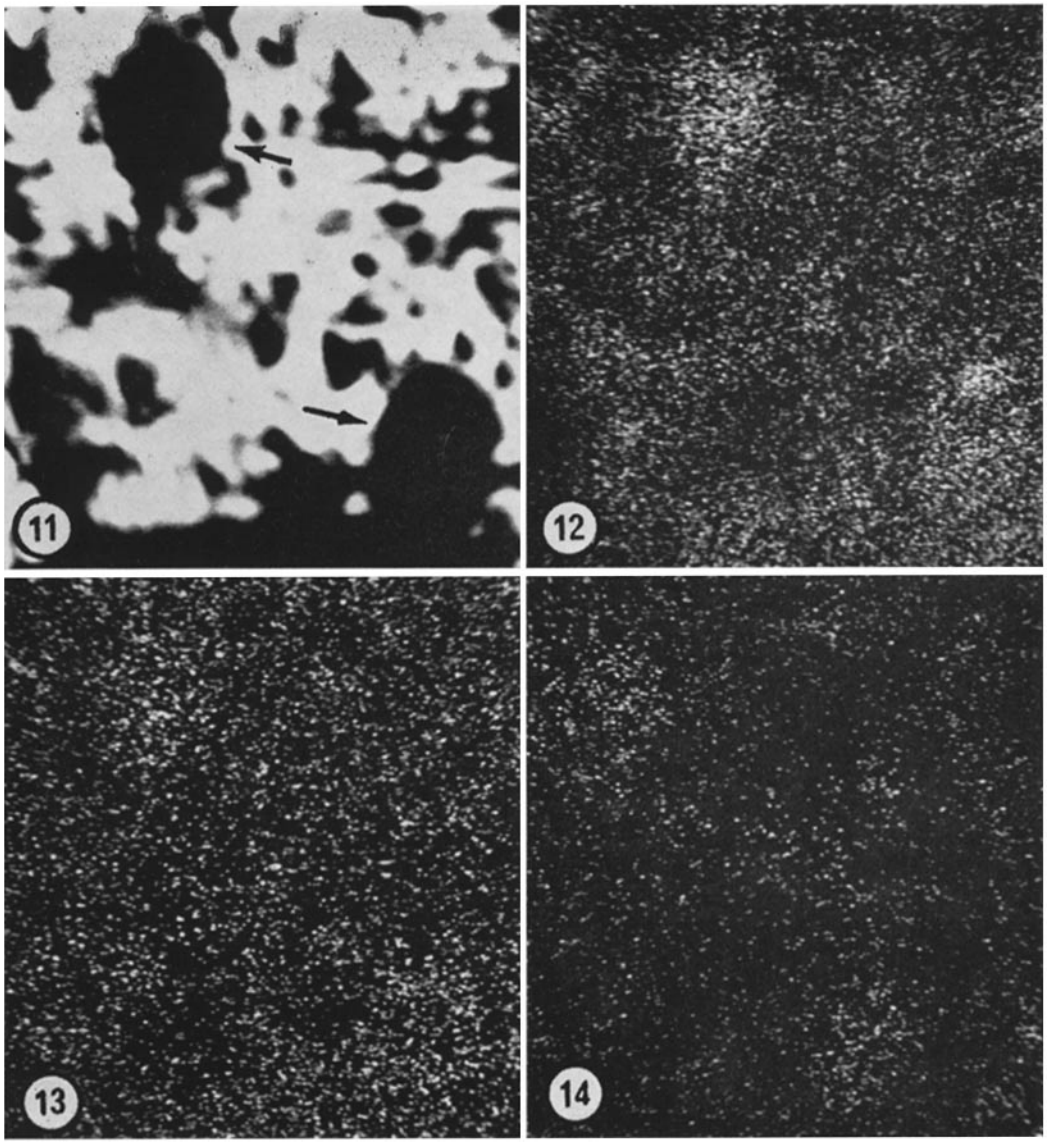

FIGURE 11 Absorbed electron image taken with the microprobe from a thick 1 μ section of rat liver fixed in potassium pyroantimonate. Two hepatocyte nuclei (arrows) are outlined, and several discrete masses of different sizes are discernible in the cytoplasm. × 2,700.

FIGURE 12 The image for the Lα_1-emission wavelength of antimony on the same area of the section shown in Fig. 11. × 2,700.

FIGURE 13 The image for the Kα_1-emission wavelength of sodium on the same area of the section shown in Figs. 11 and 12. × 2,700.

FIGURE 14 The image for the Kα_1-emission wavelength of calcium on the same area of the section shown in Figs. 11 and 12. × 2,700.

outlines of two maize nucleoli and of the cellulose walls are specially evident. In Fig. 11, two hepatocyte nuclei are outlined lying in the cytoplasm in which several discrete masses of different sizes are also discernible. These topographies can be visualized in more detail in Figs. 1 and 3, which show similar images through the electron microscope. However, the field analyzed by the probe is not identical with the area shown in the electron micrographs of Figs. 1 and 3 (e.g., the schizogenous space of Fig. 1 is not apparent in Fig. 7).

Figs. 8 and 12 show the antimony $L\alpha_1$ -emission image of the same specimens. The white specks are clearly distributed at the sites of the maize nucleoli and cellulose walls and, in the rat liver, they are found concentrated over the nuclei as well as in the cytoplasm. Evidently, the antimony distribution closely corresponds to the electron-opaque deposits as observed with the electron microscope.

Figs. 9, 10, 13, and 14 show the $K\alpha_1$-emission of the lighter elements magnesium, calcium, and sodium. The distribution of these cations corresponded to that of the antimony; this is the direct proof for the presence of those cations in the antimonate deposits and indicates that the insoluble antimonate salts were originated by a precipitation reaction with the cellular cations during the fixation process. Potassium was detected by the probe in the antimonate precipitates, a fact which indicates either a certain amount of potassium pyroantimonate that resisted the washing procedure, a coprecipitation phenomenon, or a complex chemical composition of the precipitate.

As indicated under Methods, the different micrographs are not quantitatively comparable; the relative proportions of the different cations at several loci in the sections have not been determined.

Control tissues fixed in either osmium tetroxide or aldehydes, washed with distilled water, and immersed thereafter in potassium pyroantimonate failed to show the presence of any of the lighter atomic species while they revealed only traces of antimony. This result correlates with the absence of electron-opaque deposits as observed with the electron microscope.

DISCUSSION

The present paper describes the usefulness of potassium pyroantimonate as a fixative (*alone*, without addition of any conventional fixative); the main point demonstrated is that pyroantimonate fixation of living cells produces massive precipitates of the insoluble salts of calcium, magnesium, and sodium inside the cells and tissues and a strikingly good preservation of general cell morphology. This is a constantly reproducible result, and an explanation must be given for this phenomenon. However, the exact reason(s) why this reagent behaves so succesfully is unknown. The same applies to another reagent which we have recently shown to immobilize the inorganic phosphate anions within the cell (2,3). Taken together, these results leave no doubt that the fixation procedures employed preserve a large amount of diffusible cellular electrolytes which are not retained by the conventional fixatives.

The question remains whether the localizations obtained reflect the in vivo sites. The fact that the distribution of inorganic ions is similar in a naturally dehydrated tissue (i.e., the radicle of ungerminated seeds as compared with the growing root; see Figs. 1 and 2) strongly supports the validity of the localizations obtained. Furthermore, other experimental evidence indicates that when diffusion of the soluble ions occurs it is in the outward direction, i.e., out of the nuclei and cells (and out of the tissue) leading to a loss of the electrolytes; this is the case, for instance, when another reagent—which does not affect precipitation in the test tube—is added to the potassium pyroantimonate fixative, as mentioned under Results.

Diffusion artifacts as a source of false location for the large pool of inorganic orthophosphate inside the nucleolus and nucleus have been eliminated (2), and a relatively high concentration of cations as counterions was predicted (2, 3). The fact that significant amounts of inorganic cations have now been localized at those same sites with the use of a completely different fixative also supports the contention that the electron-opaque deposits seen through the electron microscope truly represent the sites at which important amounts of electrolytes are concentrated in the living cell.

The absence of cation-antimonate precipitates at sites of high DNA content as found in the present work is at variance with the intranuclear locations described by Spicer et al. (10) using Komnick's pyroantimonate–osmium tetroxide fixative; on the other hand, several authors, using the latter procedure, either found the antimonate deposits

only in the interchromatin regions of the nucleus (e.g., Fig. 8 in reference 11) or failed to show appreciable amounts of precipitate inside the nuclei. In the tissues tested in the present work (i.e., rat liver and mazie roots), the amount of antimonate precipitated within the cells—and including their nuclei—was much greater after fixation in potassium pyroantimonate alone than when Komnick's procedure was used.

The large extent of complexing of cations in living tissues—and inside the cells—is a very well established fact, and the presence of ion-binding substances is strongly indicated (15). The present results demonstrates that the inorganic cations are present in both the cytoplasm and nucleus, and furthermore, that the distribution inside the nucleus is not homogeneous. The nucleolar boundary is quite sharply delimited by the precipitates and shows a high concentration of inorganic cations (Figs. 1–4) and inorganic orthophosphate anions (2, 3); this requires an explanation since there is no membrane at the interphase with the nucleoplasm. Accumulation of electrolytes inside the nucleoli could be due to the existence of ion-binding substances. This possibility could be considered either as a "binder" for the phosphate anion or for a cation(s), which then binds the phosphate ion. Some experimental evidence supports such an expectation. Studzinski (16) reported that the nucleolus of ethanol-fixed cells has a striking affinity for zinc and that a basic protein component(s) is responsible for this metal binding; other cations apparently have not been tried.

It is conceivable that in the cytoplasm as well as in the walls of the blood vessels (Fig. 3) the inorganic cations are largely held by fixed anionic charges (e.g., macromolecules such as RNA, acidic polysaccharides, etc.). The same could apply for the nucleus, since the pattern of inorganic cation distribution correlates with that of the ribonucleoprotein particles (Figs. 4 and 5, and reference 14). However, the accumulation of cations in the nucleus and nucleolus is noteworthy because of the coexistence of a large pool of inorganic phosphate anions at these sites (2, 3), a situation apparently not encountered in the cytoplasm. As suggested before (2, 3), the absence of mature (cation-bound) ribosomes in the nucleolus and nucleus (14, 17–19) could be due, at least partially, to an inorganic phosphate chelation of divalent cations, inasmuch as magnesium and calcium have now been demonstrated at those same sites along with the ribonucleoprotein particles.

A point to be stressed is the demonstration of the cell nucleus as an intracellular ionic compartment, which is in line with some reports in the literature strongly suggesting that the nucleus is involved in the accumulation of a number of electrolytes (see references 3, 20). However, we do not have any evidence on the exact mechanism of entrance—and exit—of phosphate anions and inorganic cations in the nucleus of the intact cell. All these ions are compartmentalized inside the nucleus and are apparently in a loosely "bound" state, i.e., they probably should not produce great osmotic alterations (which is in line with some experimental evidence; see reference 20).

The high intranuclear level of inorganic cations and orthophosphate anions certainly could affect the latency of enzymes (e.g., nucleases; see reference 19) as well as the association and dissociation of nucleic acids with respect to proteins, a fact which suggests that regulation of the ionic intranuclear environment may be involved in genetic regulatory mechanisms.

This investigation was supported by a grant from the Consejo Nacional de Investigaciones Cientìficas y Técnicas, Argentine. Dr. Tandler is an established Investigator of the CNICT and from the Instituto Fitotécnico de Santa Catalina, Argentine. Dr. Sanchis is from the Department of Ciencias Biológicas, Facultad de Farmacia y Bioquímica, Buenos Aires, Argentina.

The authors wish to express their thanks to Mr. Tulio Palacios for assistance in the operation of the microanalyzer.

Received for publication 30 September 1969, and in revised form 10 December 1969.

Note Added in Proof: In collaboration with Dr. A. L. Kierszenbaum (manuscript in preparation), the pattern of insoluble antimonate precipitation was studied in mouse testis fixed in potassium pyroantimonate. The results obtained with this technique confirmed the absence of cation-antimonate precipitates in sites of high DNA content, i.e., the condensed chromatin in the nuclei of mature spermatids and the heterochromatin masses in Sertoli's cells. The antimonate precipitate always appeared dispersed between the masses of condensed chromatin, except in the nuclei of mature spermatids which did not show any sign of antimonate deposition.

REFERENCES

1. MAHLER, H. R., and E. H. CORDES. 1967. Biological Chemistry. Harper & Row, New York, and John Weatherhill, Inc., Tokyo.
2. TANDLER, C. J., and A. J. SOLARI. 1969. Nucleolar orthophosphate ions. Electron microscope and diffraction studies. *J. Cell Biol.* **41**:91.
3. LIBANATI, C. M., and C. J. TANDLER. 1969. The distribution of the water-soluble inorganic orthophosphate ions within the cell: Accumulation in the nucleus. Electron probe microanalysis. *J. Cell Biol.* **42**:754.
4. KOMNICK, H. 1962. Elektronenmikroscopische Lokalisation von Na^+ und Cl^- in Zellen und Geweben. *Protoplasma.* **55**:414.
5. KOMNICK, H., and U. KOMNICK. 1963. Elektronen mikroscopie Untersuchungen zur Funktionellen Morphologie des Ionentransportes in der Salzdrüse von *Laurus argentatus*. *Z. Zellforsch. Mikrosk. Anat.* **60**:163.
6. KAYE, G. I., J. D. COLE, and A. DONN. 1965. Electron microscopy: Sodium localization in normal and ouabain-treated transporting cells. *Science (Washington).* **150**:1167.
7. KAYE, G. I., H. O. WHEELER, R. T. WHITLOCK, and N. LANE. 1966. Fluid transport in the rabbit gall bladder. *J. Cell Biol.* **30**:237.
8. NOLTE, A. 1966. Elektronenmikroscopische Nachweis und die Lokalisation von Natrium$^+$ und Chlorionen$^-$ in proximalen Tubulusepithelel der Rattenniere. *Z. Zellforsch. Mikrosk. Anat.* **72**:562.
9. ZADUNAISKY, J. A. 1966. The location of sodium in the transverse tubules of skeletal muscle. *J. Cell Biol.* **31**:C11.
10. SPICER, S. S., J. H. HARDIN, and W. B. GREENE. 1968. Nuclear precipitates in pyroantimonate osmium tetroxide–fixed tissues. *J. Cell Biol.* **39**:216.
11. BULGER, R. E. 1969. Use of potassium pyroantimonate in the localization of sodium ions in rat kidney tissue. *J. Cell Biol.* **40**:79.
12. LANE, B. P., and E. MARTIN. 1969. Electron probe analysis of cationic species in pyroantimonate precipitates in Epon-embedded tissue. *J. Histochem. Cytochem.* **17**:102.
13. LEGATO, M. J., and G. A. LANGER. 1969. The subcellular localization of calcium ion in mammalian myocardium. *J. Cell Biol.* **41**:401.
14. MONNERON, A., and W. BERNHARD. 1969. Fine structural organization of the interphase nucleus in some mammalian cells. *J. Ultrastruct. Res.* **27**:266.
15. LING, G. N. 1962. A physical theory of the living state. Blaisdell Publishing Co., New York.
16. STUDZINSKI, G. P. 1965. Selective binding of zinc by basic proteins of the HeLa cell nucleolus. *J. Histochem. Cytochem.* **13**:365.
17. PENMAN, S. 1966. RNA metabolism in the HeLa cell nucleus. *J. Mol. Biol.* **17**:117.
18. ROGERS, M. E. 1968. Ribonucleoprotein particles in the amphibian oocyte nucleus. *J. Cell Biol.* **36**:421.
19. LIAU, M. C., and R. P. PERRY. 1969. Ribosome precursor particles in nucleoli. *J. Cell Biol.* **42**:272.
20. SIEBERT, G., and G. B. HUMPHREY. 1965. Enzymology of the nucleus. *Advan. Enzymol.* **27**:239.